Effect of inertia on film flow over oblique and three-dimensional corrugations

Haoxiang Luo[a] and C. Pozrikidis[b]
Department of Mechanical and Aerospace Engineering, University of California, San Diego, La Jolla, California 92093-0411

(Received 1 April 2006; accepted 9 June 2006; published online 28 July 2006; publisher error corrected 13 November 2006)

The gravity-driven flow of a liquid film down an inclined plane wall with small-amplitude two-dimensional oblique or three-dimensional doubly periodic corrugations is investigated for finite Reynolds numbers. The film surface may exhibit constant or variable surface tension due to an insoluble surfactant. The key idea is to express the wall geometry as a Fourier series, and then reconstruct the three-dimensional flow in terms of the individual two-dimensional transverse and unidirectional flows over the constituent oblique two-dimensional corrugations. Three-dimensional corrugations may either reduce or amplify the surface deformation with respect to their two-dimensional counterparts due to the simultaneous effect of the constituent oblique components on the effective wave number, capillary number, and Reynolds number. © *2006 American Institute of Physics*. [DOI: 10.1063/1.2227050]

In recent papers, Wang[1] and the present authors[2] considered Stokes flow down an inclined wall with small-amplitude three-dimensional periodic corrugations in the possible presence of an insoluble surfactant. In the formulation of Luo and Pozrikidis,[2] the three-dimensional flow was synthesized from elementary constituents involving unidirectional and two-dimensional flow. In this Brief Communication, the analysis is extended to nonzero Reynolds numbers. Previously, Bontozoglou and co-workers[3–5] demonstrated that inertia may cause a kind of resonance in two-dimensional film flow with a clean interface, wherein the surface amplitude becomes much larger than the amplitude of a sinusoidal wall. A similar behavior is expected to occur in three-dimensional flow.

Figure 1 schematically illustrates the flow under consideration. The base plane of the wall in the absence of corrugations located at $z=0$ is inclined at an angle θ_0 with respect to the horizontal. The Cartesian components of the acceleration of gravity vector are $\mathbf{g}=g(\sin\theta_0, 0, -\cos\theta_0)$. The wall geometry is described by the function $z=z_w(x,y)$, and the periodicity of the corrugations is determined by two base vectors, $\mathbf{l}_1$ and $\mathbf{l}_2$, that are parallel to the xy plane and are defined such that $z_w(\mathbf{w})=z_w(\mathbf{w}+i\mathbf{l}_1+j\mathbf{l}_2)$, where $\mathbf{w}=(x,y)$, and i and j are two integers. The wall function $z_w(x,y)$ may be expanded in a two-dimensional Fourier series,

$$z_w(x,y)=\sum_{n=-\infty}^{\infty}\sum_{m=-\infty}^{\infty} c_{nm}e^{i(n\mathbf{k}_1+m\mathbf{k}_2)\cdot\mathbf{w}}, \tag{1}$$

where c_{nm} are complex expansion coefficients, i is the imaginary unit, and $\mathbf{k}_1$, $\mathbf{k}_2$ are the reciprocal wavelength vectors satisfying $\mathbf{k}_i\cdot\mathbf{l}_j=2\pi\delta_{ij}$. A two-dimensional wall geometry consisting of streamwise, spanwise, or oblique corrugations arises for specific choices of the expansion coefficients, c_{nm}.

The motion of the fluid is governed by the Navier–Stokes equation and the continuity equation,

$$\rho(\mathbf{u}\cdot\nabla)\mathbf{u}=-\nabla p+\mu\nabla^2\mathbf{u}+\rho\mathbf{g}, \quad \nabla\cdot\mathbf{u}=0, \tag{2}$$

where μ and ρ are the liquid viscosity and density, $\mathbf{u}=(u,v,w)$ is the velocity, and p is the pressure. The velocity is required to satisfy the no-slip and no-penetration boundary conditions over the wall, $\mathbf{u}=\mathbf{0}$, and the hydrodynamic traction $\mathbf{f}$ is required to satisfy the dynamic boundary condition $\mathbf{f}=\boldsymbol{\sigma}\cdot\mathbf{n}=(2\gamma\kappa-p_a)\mathbf{n}-\nabla_s\gamma$, over the film surface, where $\boldsymbol{\sigma}$ is the Newtonian stress tensor, γ is the position-dependent surface tension, $\mathbf{n}$ is the unit normal vector pointing into the film, $\nabla_s\equiv(\mathbf{I}-\mathbf{nn})\cdot\nabla$ is the surface gradient, $\kappa\equiv\frac{1}{2}\nabla_s\cdot\mathbf{n}$ is the mean curvature of the free surface, and p_a is the ambient pressure. The surface tension, γ, is a function of the surfactant concentration, Γ, whose distribution is determined by the convection–diffusion transport equation $\nabla_s\cdot(\Gamma\mathbf{u}_s)=D_s\nabla_s^2\Gamma$, where $\mathbf{u}_s$ is the tangential velocity, and D_s is the surfactant diffusivity.[6] For small deformations, a linear relationship may be assumed between the surface tension and the surfactant concentration, $\gamma=\gamma_0(1+\mathrm{Ma}(1-\Gamma/\Gamma_0))$, where Γ_0 is a reference concentration corresponding to the surface tension γ_0, and Ma is the Marangoni number.[7,8]

In the simplest possible configuration, the wall exhibits small-amplitude sinusoidal undulations described by the real or imaginary part of the complex function $z_w(x,y)=\epsilon he^{i(\mathbf{k}_1+\mathbf{k}_2)\cdot\mathbf{w}}$, where ϵ is a dimensionless coefficient whose magnitude is much less than unity, and h is the mean film thickness. Setting $\mathbf{k}_1=(k_{11},k_{12})$, and $\mathbf{k}_2=(k_{21},k_{22})$, we obtain $z_w(x,y)=\epsilon he^{i(\alpha_1x+\alpha_2y)}$, where $\alpha_1=k_{11}+k_{21}$ and $\alpha_2=k_{12}+k_{22}$. Thus, the wall geometry is an oblique harmonic wave with wave number $\hat{k}=\sqrt{\alpha_1^2+\alpha_2^2}$ whose ridges are inclined at an angle θ with respect to the x axis, where $\tan\theta=-\alpha_1/\alpha_2$ and $\theta\in[0,\pi)$. The flow over the oblique wave can be further

[a]Electronic mail: hluo@gwu.edu
[b]Electronic mail: cpozrikidis@ucsd.edu

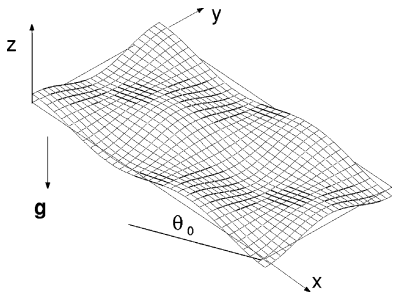

FIG. 1. Schematic illustration of film flow down an inclined wall with three-dimensional periodic corrugations.

decomposed into a transverse flow perpendicular to the ridges, and a parallel flow along the ridges. To implement this decomposition, we introduce the oblique coordinates $\xi=x\sin\theta-y\cos\theta$, $\eta=x\cos\theta+y\sin\theta$, designed so that the ridges are perpendicular to the ξ axis and parallel to the η axis. The wall geometry is then described by $z_w(\xi)=\epsilon h e^{i\hat{k}\xi}$. The velocity components in the oblique coordinates (ξ,η,z) are designated as $(\hat{u},\hat{v},\hat{w})$.

The zeroth-order flow is described by the flat-film Nusselt solution for a plane wall.[2] Performing a standard perturbation analysis, we find that the first-order flow satisfies the governing equations

$$\rho\left(\hat{u}^{(0)}\frac{\partial\hat{u}^{(1)}}{\partial\xi}+\hat{w}^{(1)}\frac{\partial\hat{u}^{(0)}}{\partial z}\right)=-\frac{\partial p^{(1)}}{\partial\xi}+\mu\hat{\nabla}^2\hat{u}^{(1)},$$

$$\rho\left(\hat{u}^{(0)}\frac{\partial\hat{w}^{(1)}}{\partial\xi}\right)=-\frac{\partial p^{(1)}}{\partial z}+\mu\hat{\nabla}^2\hat{w}^{(1)}, \tag{3}$$

$$\rho\left(\hat{u}^{(0)}\frac{\partial\hat{v}^{(1)}}{\partial\xi}+\hat{w}^{(1)}\frac{\partial\hat{v}^{(0)}}{\partial z}\right)=\mu\hat{\nabla}^2\hat{v}^{(1)},$$

where the superscripts designate the order of the solution, and $\hat{\nabla}^2=\partial^2/\partial^2\xi+\partial^2/\partial^2 z$. The first and second equations in (3) govern the transverse flow in the ξz plane, while the third equation governs the unidirectional flow along the η axis; all velocity components are independent of η. The film surface is described by the function $z_s(\xi)=h+\epsilon s(\xi)$. The linearized kinematic compatibility condition at the free surface requires

$$\hat{u}^{(0)}\frac{\partial s}{\partial\xi}-\hat{w}^{(1)}=0, \tag{4}$$

at $z=h$, and the linearized no-slip and no-penetration conditions at the wall require

$$\hat{u}^{(1)}+\frac{\partial\hat{u}^{(0)}}{\partial z}he^{i\hat{k}\xi}=0,\quad \hat{v}^{(1)}+\frac{\partial\hat{v}^{(0)}}{\partial z}he^{i\hat{k}\xi}=0,\quad \hat{w}^{(1)}=0, \tag{5}$$

at $z=0$. Linearizing the dynamic interfacial condition yields the following shear and normal stress surface conditions:

$$\mu\left(\frac{\partial\hat{u}^{(1)}}{\partial z}+\frac{\partial\hat{w}^{(1)}}{\partial\xi}\right)+\mu\frac{\partial^2\hat{u}^{(0)}}{\partial z^2}s=\frac{\partial\gamma^{(1)}}{\partial\xi},$$

$$\frac{\partial\hat{v}^{(1)}}{\partial z}+\frac{\partial^2\hat{v}^{(0)}}{\partial z^2}s=0,\quad -p^{(1)}+2\mu\frac{\partial\hat{w}^{(1)}}{\partial z}-\frac{\partial p^{(0)}}{\partial z}s=\gamma_0\hat{\nabla}^2 s, \tag{6}$$

evaluated at $z=h$. Linearizing the surfactant transport equation, we obtain

$$\hat{u}^{(0)}\frac{\partial\Gamma^{(1)}}{\partial\xi}-\Gamma_0\frac{\partial\hat{w}^{(1)}}{\partial z}=D_s\hat{\nabla}^2\Gamma^{(1)} \tag{7}$$

evaluated at $z=h$. The two-dimensional transverse flow determines the shape of the interface and surface distribution of the surfactant, independent of the parallel cross-flow. In contrast, the cross-flow is affected by the two-dimensional flow through the shape of the interface, as can be seen in the second equation in (6), as well as by the nonlinear coupling between the first-order perturbation term $\hat{w}^{(1)}$ and unperturbed term $\partial\hat{v}^{(0)}/\partial z$ in the third equation of (3).

To solve the linear equations, we express the first-order perturbations as

$$s=Ahe^{i\hat{k}\xi},\quad \Gamma^{(1)}=C\Gamma_0 e^{i\hat{k}\xi},\quad \gamma^{(1)}=D\gamma_0 e^{i\hat{k}\xi},$$

$$\psi^{(1)}=\hat{U}hf(\check{z})e^{i\hat{k}\xi},\quad \hat{u}^{(1)}=\hat{U}f'(\check{z})e^{i\hat{k}\xi}, \tag{8}$$

$$\hat{v}^{(1)}=\hat{V}r(\check{z})e^{i\hat{k}\xi},\quad \hat{w}^{(1)}=-i\hat{k}\hat{U}hf(\check{z})e^{i\hat{k}\xi},$$

where $\check{z}=z/h$, $\hat{U}=U\sin\theta$ and $\hat{V}=U\cos\theta$ are the unperturbed surface velocities in the ξ and η directions, respectively, $U=\rho g h^2\sin\theta_0/(2\mu)$ is the unperturbed surface velocity along the x axis, and A,C,D are nondimensional complex amplitudes. Eliminating the pressure from the first and second equations in (3) by taking the curl, and then substituting expressions (8), we derive the Orr–Sommerfeld equation

$$\mathcal{D}^2 f(\check{z})=(i\check{k})\mathrm{Re}_\xi\left[\check{z}(2-\check{z})\frac{\mathrm{d}^2 f}{\mathrm{d}\check{z}^2}+(2-\check{z}(2-\check{z})\check{k}^2)f\right], \tag{9}$$

where $\mathcal{D}=\mathrm{d}^2/\mathrm{d}\check{z}^2-\check{k}^2$, $\check{k}=\hat{k}h$, and $\mathrm{Re}_\xi=\rho\hat{U}h/\mu$ is the effective Reynolds number of the two-dimensional flow. The accompanying boundary conditions are

$$A+f(\check{z}=1)=0,\quad f'(\check{z}=0)=-2,\quad f(\check{z}=0)=0,$$

$$f'''-3\check{k}^2 f'+2i\check{k}\tau f=(i\check{k})\mathrm{Re}_\xi f',\quad \text{at}\quad \check{z}=1,$$

$$f''+(\check{k}^2+2)f-\frac{4\pi^2 i}{\mathrm{Ca}_\xi\check{k}}D=0,\quad \text{at}\quad \check{z}=1, \tag{10}$$

$$\left(1-\frac{2\pi i}{\mathrm{Pe}}\right)C+2f'(\check{z}=1)=0,\quad D+\mathrm{Ma}\,C=0,$$

where $\tau\equiv\cot\theta_0/\sin\theta+2\pi^2/\mathrm{Ca}_\xi$, $\mathrm{Ca}_\xi=(\mu\hat{U}/\gamma_0)(\hat{l}/h)^2$ is the effective capillary number, $\hat{l}=2\pi/\hat{k}$ is the effective wavelength, and $\mathrm{Pe}=\hat{l}\hat{U}/D_s$ is the surface Péclet number. When $\theta=\pi/2$ and $\mathrm{Ma}=0$, Eqs. (9) and (10) reduce to those presented in Ref. 3. The counterpart of the fifth equation of (10)

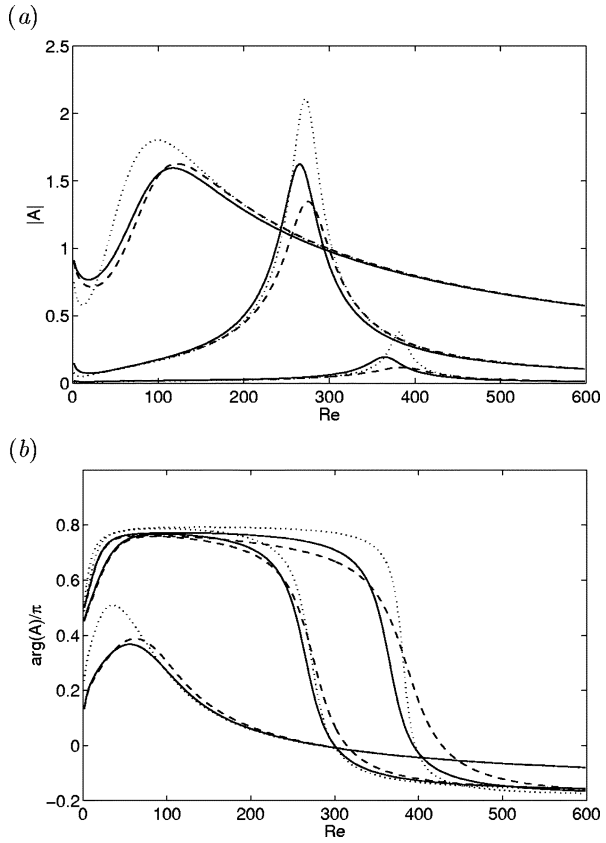

FIG. 2. (a) Surface amplitude and (b) phase shift of a water film down a two-dimensional corrugated wall for l=0.001 m (right), 0.002 (middle), 0.005 (left), and Ma=0 (dotted lines), 0.1 (dashed lines), 1 (solid lines).

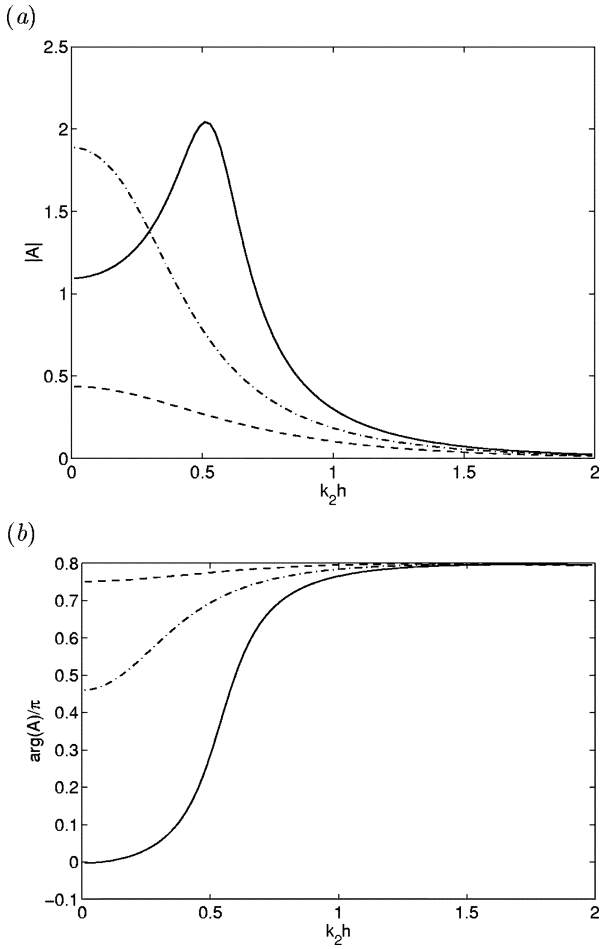

FIG. 3. (a) Surface amplitude and (b) phase shift of film flow down a three-dimensional wavy wall for Re=225 (dashed lines), 270 (dashed-dotted lines), and 300 (solid lines).

in Ref. 3 displays an erroneous sign. Equations (9) and (10) were solved and the constants A, C, D are simultaneously evaluated using a Chebyshev tau method (e.g., Refs. 9–11). After the transverse flow has been obtained, the unidirectional flow is calculated by solving the equation

$$r''(\check{z}) - \check{k}^2 r(\check{z}) = (i\check{k})\mathrm{Re}_\xi[\check{z}(2-\check{z})r(\check{z}) - 2(1-\check{z})f(\check{z})], \quad (11)$$

subject to the second condition in (6) and the no-slip condition expressed by the second equation in (5), requiring $r'(\check{z}=1)=2A$ and $r(\check{z}=0)=-2$. The solution is also found using the Chebyshev tau method. In summary, the structure of the flow down the oblique wall depends on the reduced wave number $\check{k}$, inclination angle θ_0, obliqueness angle θ, Reynolds number Re_ξ, capillary number Ca_ξ, Marangoni number Ma, and Pe determining the surfactant diffusivity. Alternatively, we may define a Reynolds number and a capillary number that are independent of the orientation of the oblique wall, $\mathrm{Re}=\rho U h/\mu$, $\mathrm{Ca}=\mu U/\gamma_0$.

As a preliminary, we consider the deformation of a two-dimensional film of water down a wall with transverse corrugations along the y axis described by the function $z_w(x) = \epsilon h \cos(kx)$ at temperature 20 °C, also considered in Ref. 3. Figure 2 shows the surface amplitude and phase shift with respect to the wall for $\theta_0=\pi/6$, wavelength l=0.001, 0.002, 0.005 m, Ma=0, 0.1, 1, and Re ranging from 0 to 600. As in Ref. 3 to change the Reynolds number we vary the film thickness. The capillary number Ca varies from 0 to 0.013. The clean surface cases, Ma=0, are represented by the dotted lines in the graphs. As reported in Ref. 3 the surface amplitude exhibits a resonance in a narrow band of Reynolds numbers. The maximum amplitude of the surface is somewhat lower than that reported in Ref. 3 due to the aforementioned difference in sign. In addition, we find that the phase shift does not exhibit a discontinuous jump at resonance as reported in Ref. 3. Rather, for l=0.001 and 0.002 m, the phase shift exhibits a smooth transition approximately from 0.8π to -0.2π, reducing by almost 180°. The overall trend of the phase shift is consistent for different wavelengths.

The effect of the surfactant is illustrated in Fig. 2(a). For all three wavelengths, the surface amplitude at resonance is significantly reduced by the surfactant, while the resonant Reynolds number is shifted by a small amount. The effect of the surfactant is nonmonotonic. For example, in the cases of l=0.001 and 0.002 m, the surface amplitude for Ma=1 is greater than that for Ma=0.1. Further increasing the Marangoni number in these three cases does not change the surface deformation significantly. The influence of Ma on the phase shift is most pronounced near the resonance Re where the transition is smoothed out by the surfactant. In the case of Stokes flow, it is known that the surfactant amplifies the

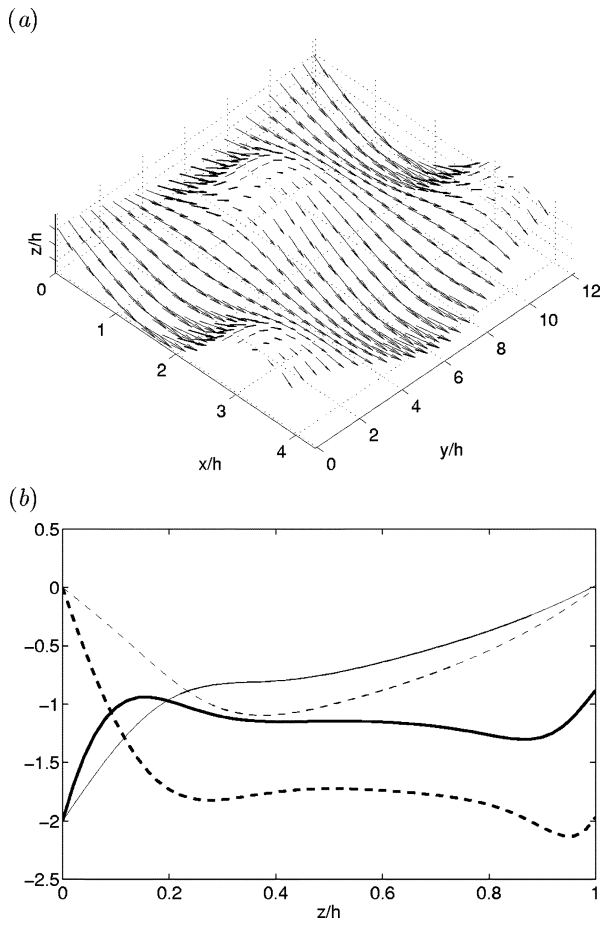

FIG. 4. (a) Film surface and surface velocity field for flow down a three-dimensional corrugated wall. (b) Profiles of functions $f'(\check{z})$ (thick lines) and $r(\check{z})$ (thin lines). The imaginary parts are shown as dashed lines.

surface deformation.[12] In Fig. 2(a), we can see the reversing of the role of the surfactant in the cases of $l=0.002$ and 0.005 m. As Re is reduced from the resonant value to zero, the surface amplitude for higher Ma gradually surpasses the corresponding amplitude for lower Ma.

Next, we consider flow down a three-dimensional wall described by $z_w=\epsilon h\cos(k_1x)\cos(k_2y)$, where k_1 and k_2 are specified wave numbers. Cursory inspection reveals that this shape function can be expressed as a linear combination of the two cosine Fourier modes, $\cos(k_1x+k_2y)$ and $\cos(k_1x-k_2y)$, representing oblique waves that are symmetric about the x axis with equal oblique wave numbers, $\hat{k}=\sqrt{k_1^2+k_2^2}$, and identical amplitudes. The surface of the deformed film is described by $z_s(x,y)=h+\epsilon|A|h\cos[k_1x+\arg(A)]\cos(k_2y)$, where the complex amplitude, A, is computed precisely as discussed previously for either one of the two Fourier modes. As expected on geometrical reasoning, the surface deformation is displaced with respect to the wall in the streamwise direction by an amount that is determined by $\arg(A)$. Luo and Pozrikidis[2] found that, in Stokes flow, the three-dimensional corrugations reduce the surface deformation relative to that of the corresponding two-dimensional corrugations, by increasing the effective wave number and reducing the effective capillary. When inertia is present, in addition to increasing $\hat{k}$ and decreasing Ca_ξ, the effective Reynolds number Re_ξ is also reduced by the three-dimensional corrugations. We have seen that the Reynolds number has a non-uniform effect on the surface deformation in two-dimensional flow, and properly tuning Re may cause large amplification of the surface wave. Accordingly, the overall effect of the three-dimensional corrugations is not as easily seen as in the case of Stokes flow, the reason being that it is primarily dominated by the Reynolds number effect in the resonance range, and is determined by the balance of opposing parameters outside this range.

Figure 3 shows the amplitude and phase shift of the film surface for $k_1h=\pi/2$, $\theta_0=\pi/6$, and Ma=0, over a range of k_2h. The Reynolds number based on the surface velocity of the assembled unidirectional flow is Re=225, 270, or 300, and the corresponding capillary number is Ca=0.0069, 0.0078, or 0.0083. For Re=225, and 270, increasing k_2h reduces the surface amplitude; for Re=300, increasing k_2h causes a large oscillation of the surface deformation. Clearly, the resonance condition is encountered during the increase of the transverse wave number. In all three cases, the phase shift rises monotonically with k_2h within the parameters range considered.

Figure 4(a) illustrates the velocity field and the free surface shape for Re=300 and $k_2h=0.51$. The dimensionless amplitude of the free surface is $|A|=2.04$, and the phase-shift is $\arg(A)=0.31\pi$. The flow is symmetric about the $y=0$ plane, with the velocity vectors generally following the wavy surface in the x direction. Small deviations in the y direction occur over the tops of the bumps. Figure 4(b) shows the profiles of the functions $f'(\check{z})$ and $r(\check{z})$ for the constituent flow components, revealing that the transverse flow exhibits significant variations near the wall and the free surface.

This research was supported by a grant provided by the National Science Foundation.

[1] C. Y. Wang, "Low Reynolds number film flow down a three-dimensional bumpy surface," J. Fluids Eng. **127**, 1122 (2005).
[2] H. Luo and C. Pozrikidis, "Gravity-driven film flow down an inclined wall with three-dimensional corrugations," Acta Mech. (in press).
[3] V. Bontozoglou and G. Papapolymerou, "Laminar flow down a wavy incline," Int. J. Multiphase Flow **23**, 69 (1997).
[4] N. A. Malamataris and V. Bontozoglou, "Computer aided analysis of viscous film flow along an inclined wavy wall," J. Comput. Phys. **154**, 372 (1999).
[5] M. Vlachogiannis and V. Bontozoglou, "Experiments on laminar film flow along a periodic wall," J. Fluid Mech. **457**, 133 (2002).
[6] C. Pozrikidis, "Interfacial dynamics for Stokes flow," J. Comput. Phys. **169**, 250 (2001).
[7] A. W. Adamson, *Physical Chemistry of Surfaces* (Wiley, London, 1990).
[8] C. Pozrikidis, "Instability of multilayer channel and film flows," Adv. Appl. Mech. **40**, 179 (2004).
[9] J. J. Dongarra, B. Straughan, and D. W. Walker, "Chebyshev tau-QZ algorithm methods for calculating spectra of hydrodynamic stability problems," Appl. Numer. Math. **22**, 399 (1996).
[10] S. A. Orszag, "Accurate solution of the Orr–Sommerfeld stability equation," J. Fluid Mech. **50**, 689 (1971).
[11] M. G. Blyth and C. Pozrikidis, "Effect of surfactant on the stability of film flow down an inclined plane," J. Fluid Mech. **521**, 241 (2004).
[12] C. Pozrikidis, "Effect of surfactants on film flow down a periodic wall," J. Fluid Mech. **496**, 105 (2003).